An Investigation of Impulsive-Maneuver Transfers from L_3, L_4 and L_5 to Earth-Orbit

Evangelina A. Evans
University of Colorado Boulder
Marcus J. Holzinger
University of Colorado Boulder

Daniel J. Scheeres
University of Colorado Boulder

ABSTRACT

Cislunar space has increasingly captivated the attention of both commercial and defense sectors, driven by ambitions to extend the operation of space-based assets into this expansive domain. The stable triangular Lagrange points, L_4 and L_5, offer diverse viewing angles of the Earth-Moon system making them prime candidates for space infrastructure and situational awareness. L_3 has commonly been overlooked for mission applications due to its distance from lunar vicinity and is thus less trafficked. While considerable attention has been devoted to transfers from Earth to the Lagrange points, notably L_1 and L_2 in preparation for Lunar Gateway, there is a growing need to explore trajectories returning from cislunar regions to Earth orbit. To effectively navigate and exploit cislunar space for this purpose, it is imperative to establish a comprehensive understanding of its astrography. This entails mapping impulsive-maneuver transfers within the Earth-Moon system from L_3, L_4 and L_5 to Earth-orbit destinations including GEO, MEO, and LEO. It is crucial to delineate criteria for evaluating the value of trajectories in this domain: delta-v and the flight duration of the transfer. Identifying common pathways is also vital for efficient space traffic management and situational awareness, akin to maritime chokepoints facilitating commerce across the high seas.

1. INTRODUCTION

Cislunar space has become a region of interest as commercial and defense sectors seek to expand the operational capabilities of space-based assets into this domain. To effectively navigate and use this region in space, its foundational astrography needs to be defined by mapping key trajectories in the Earth-Moon system [10]. However, a prerequisite for cislunar astrography requires establishing criteria for evaluating what makes a trajectory strategically valuable in the space domain.

A spacecraft's trajectory through cislunar space is heavily dependent on two factors: delta-v (velocity changes, representative of fuel-cost) and time of flight (TOF). A number of feasible trajectories can exist between two regions (or orbits) in cislunar space through the variation of these parameters. While each trajectory is defined by its own propulsive maneuvers, trajectories may travel along similar pathways or converge through a distinct region in space. Analogous to the concept of maritime chokepoints – which represent convergent lines of commerce across the high seas – identifying where and how lines of commerce exist in cislunar space is beneficial to space traffic management and space situational awareness (SSA). Additional qualifications for a strategic trajectory stem from application-based implications such as the detectability of a satellite along the trajectory and spaceflight safety [6, 5].

The Earth-Moon Lagrange points have previously been identified as key regions in cislunar space [4]. In recent years, the field has directed research of the Earth-Moon system to the L_1 and L_2 Lagrange points attributed to development of NASA's lunar gateway [7, 3, 8]. The L_1 and L_2 regions, being in lunar vicinity, are also more heavily trafficked than the triangular Lagrange points and L_3 at present. The triangular Lagrange points, L_4 and L_5, are gaining notice as strategic regions for space infrastructure and SSA due to their stability and diverse viewing geometry of the Earth-Moon system [9]. Due to their stability, these regions also offer minimal station-keeping requirements [2]. L_3 remains less studied with efforts designing two-impulse transfers from Earth to L_3 libration point orbits (LPOs) [1]. This work will further examine the lesser studied L_3, L_4 and L_5 regions.

Historically, research has limited the direction of travel along cislunar trajectories as departing from Earth, the common objective being to design transfers specifically from an Earth orbit to LPOs to place assets in-orbit about the Lagrange points [7, 3, 8, 9, 1]. To encompass all spaceflight applications, including those that are modernly achievable or futuristic such as crewed missions and asteroid mining, trajectories returning from cislunar regions to Earth-orbit must be researched as well. The results of recent work have also focused on analyzing transfers between specified orbits or orbit families (e.g. For lunar gateway, a geostationary transfer orbit [GTO] to near rectilinear halo orbit [NRHO]) [7]. Developing a rudimentary understanding of cislunar astrography will require more generalized, high-level results that analyze trajectories traveling from various cislunar regions to the domain of Earth-orbit (all orbits extending out to and including geosynchronous Earth orbit [GSO]), not just case-based orbit-to-orbit transfers.

In this work, trajectories from the Earth-Moon L_3, L_4, and L_5 equilibrium points to Earth-orbit are modeled according to the Circular Restricted Three-Body Problem (CR3BP) dynamics. Given an initial impulsive maneuver at Lagrange points, trajectories are numerically integrated for a one-month period. Trajectories with a perigee intersecting the domain of Earth-orbit are flagged as trajectories of interest. A second impulsive maneuver is then used as a circularizing burn to inject into Earth-orbit at the perigee altitude, pro- versus retro-grade direction is determined and corresponds to the direction of the velocity vector of the incoming trajectory at perigee. Results will discuss the tradespace between delta-v and TOF for trajectories transferring from the Lagrange points to the common Earth-orbits of GEO, half-GEO, and LEO. Through a survey of the trajectories, we identify the minimum-delta-v and minimum-TOF members and determine strategic attributes of the pathways traveled through space. Through these methods of analysis, we will contribute to the mapping of strategic regions of interest within cislunar space, a critical step in defining the foundations of astrography for the Earth-Moon system.

2. BACKGROUND

2.1 Circular Restricted Three-Body Problem

Spacecraft motion is influenced by several (arguably infinite) gravitational bodies and external perturbing forces. The Circular Restricted Three-Body Problem (CR3BP) is a simplified dynamics model that defines the orbital motion of a massless particle moving under the gravitational influence of two primary bodies modeled as finite point masses m_1 and m_2. This three-body system is characterized by the mass ratio of the system $\mu = m_2/(m_1+m_2)$ where typically $m_2 \leq m_1$ is standard convention. For the Earth-Moon system $\mu \approx 0.01215$. The two primaries are assumed to move along circular orbits about their barycenter. This barycenter defines the origin of a uniformly rotating plane. The x-axis of the coordinate system points from m_1 to m_2, the z-axis points in the direction of angular momentum vector for the rotating plane, and the y-axis completes a right-handed set.

Nondimensionalization for the CR3BP defines the distance between the Earth and Moon as unity, the system's total mass as unity, and the system's rotation period as 2π (nondimensionalized time equivalent of one month). The computation of quantities relating to the CR3BP will be carried out using these nondimensionalized units (distance unit [DU] and time unit [TU]). Results may be reported in dimensionalized units.

The dynamics of this system are defined by the CR3BP equations of motion

$$\ddot{x} = x + 2\dot{y} - \frac{(1-\mu)(x+\mu)}{r_1^3} - \frac{\mu(x+\mu-1)}{r_2^3} \tag{1}$$

$$\ddot{y} = y - 2\dot{x} - \frac{(1-\mu)y}{r_1^3} - \frac{\mu y}{r_2^3} \tag{2}$$

$$\ddot{z} = -\frac{(1-\mu)z}{r_1^3} - \frac{\mu z}{r_2^3} \tag{3}$$

where

$$r_1 = [(x+\mu)^2 + y^2 + z^2]^{\frac{1}{2}} \tag{4}$$

$$r_2 = [(x-1+\mu)^2 + y^2 + z^2]^{\frac{1}{2}}. \tag{5}$$

In the planar formulation of the CR3BP, it is assumed that all motion remains in the x-y plane so that the z-components of position, velocity, and acceleration are set to zero and excluded. The planar state vector is therefore defined as

$X(t) = [x,\ y,\ \dot{x},\ \dot{y}]^T$ having an initial condition notated by $X_0 = X(0)$ (each component of the initial state vector will also follow this notation, i.e. $\dot{x}_0 = \dot{x}(0)$). Analysis described in proceeding sections of this paper will consider the planar CR3BP.

2.2 Lagrange Points

In the CR3BP, Lagrange points (LPs) are the five equilibria that exist in this dynamical systems model. They are classified as either collinear or triangular Lagrange points. The collinear Lagrange points, L_1-L_3, are located along the x-axis of the system; L_1 between the primaries, L_2 set to the outside of m_1, and L_3 set to the outside of m_2. The triangular Lagrange points, L_4 and L_5, are located on a unity equilateral triangle formed by the Earth, Moon, and respective Lagrange point. The layout of the Earth-Moon system's LPs is shown in Figure 1.

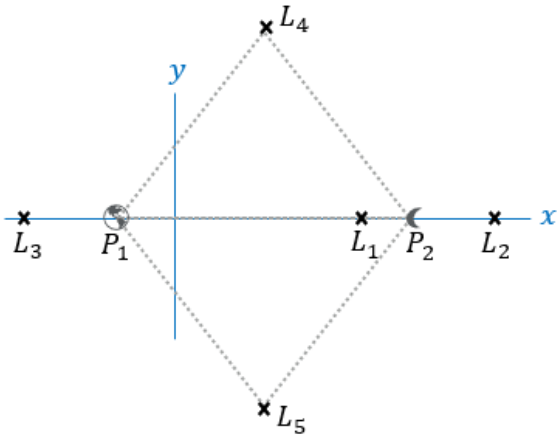

Fig. 1: Lagrange point locations in the Earth-Moon system (not to scale).

The planar state vector evaluated at a Lagrange point is written as

$$X_{LP} = [x_{LP},\ y_{LP},\ 0,\ 0]^T \tag{6}$$

where the position coordinates used for each Lagrange point are documented in Table 1 and the velocity is zero. The coordinate positions for L_4 and L_5 are found by analytically solving Eqs. 1-2 as a system of equations and L_1-L_3 are found numerically using `fsolve` in MATLAB.

LP	x_{LP}, DU	y_{LP}, DU
L_1	0.83691513	0
L_2	1.15568217	0
L_3	-1.00506265	0
L_4	$0.5-\mu$	$\sqrt{3}/2$
L_5	$0.5-\mu$	$-\sqrt{3}/2$

Table 1: Planar position coordinates for the LPs.

The planar CR3BP observes geometric symmetry about the x-axis of the rotating frame according to the coordinate transformation

$$(x, y, \dot{x}, \dot{y}, t) \Longrightarrow (x, -y, -\dot{x}, \dot{y}, -t). \tag{7}$$

As L_4 and L_5 are located across the rotating frame's x-axis, respective trajectories to and from these Lagrange points observe this transformation. For example, the spatial path followed by a trajectory departing from L_4 can be mirrored across the x-axis as a trajectory arriving to L_5. Such a pairing of trajectories is recovered by numerically integrating: (1) an initial state at L_4 forwards in time and (2) this L_4 initial state transformed through Eq. 7 (so that it becomes an initial state at L_5) backwards in time.

3. METHODS

3.1 Compute Trajectories from the Lagrange Points to Earth-Orbit

Step 1: Generate trajectories originating from the Lagrange points

Trajectories originate from a desired Lagrange point: L_3, L_4 or L_5, at which an impulsive maneuver is applied. The imparted velocity change $\Delta\bar{v}_1$ is defined by both magnitude Δv_1 and direction θ (see Figure 2) such that the initial state of a planar trajectory is $X(0) = [x_{LP},\ y_{LP},\ \Delta v_1 \cos(\theta),\ \Delta v_1 \sin(\theta)]^T$. Varying the Δv_1 and θ parameters across a range of values produces a set of initial conditions resulting in a collection of trajectories such as the collection shown in Figure 2.

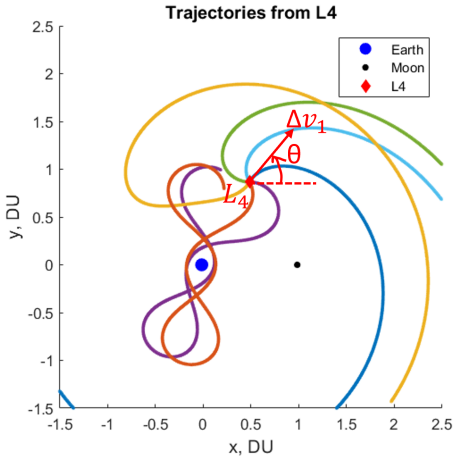

Fig. 2: Defining magnitude and direction of the initial impulsive velocity change.

In this study, the parameter values used are $\Delta v_1 \in \{0, 0.01, \ldots, 0.8\}$ DU and $\theta \in \{0, 0.01, \ldots, 360\}$ degrees. Iterating over all two-parameter combinations, as a grid search, trajectories are propagated for a duration of 2π TU, equivalent to a month-long transfer, using `ode45` in MATLAB. Trajectories impacting the Earth or Moon are terminated upon impact. Trajectories considered to have escaped the Earth-Moon system are terminated when $r > 3$ DU from the barycenter.

Step 2: Select desired Earth-orbit destinations

The Earth-orbit regimes of geosynchronous Earth orbit (GSO), medium Earth orbit (MEO), low Earth orbit (LEO) are popular destinations for active spacecraft. Each orbit regime houses an assortment of satellite-based services including telecommunications, global positioning systems, and weather monitoring.

Within each regime, we select a planar circular orbit as a desirable Earth-orbit destination for inbound trajectories from the L_3-L_5 Lagrange points: geostationary Earth orbit (GEO), half-GEO, and a 1000-km altitude LEO. The radial distances, relative to Earth's center, for each orbit are provided in Table 2.

Orbit	Radius, km
GEO	42,164
MEO	26,578
LEO	7,378

Table 2: Selected orbit radii.

Each of the selected Earth-orbits are modeled as two-body problem (2BP) solutions. The on-orbit velocity vector, v_{orbit}, is tangent to the radial position vector of the orbit relative to Earth, r_{orbit}, and its magnitude is computed by the circular velocity equation

$$v_{\text{orbit}} = \sqrt{\frac{\mu_E}{r_{\text{orbit}}}} \tag{8}$$

where $\mu_E = 3.986 * 10^5$ km^3/s^2 is the gravitational parameter of the Earth. Vectors given in the 2BP are inertial, unlike solutions of the CR3BP whose vectors are relative to the CR3BP rotating frame.

Step 3: Find Earth-orbit intersections

Along a CR3BP trajectory, the radial distance of the spacecraft (sc) relative to the Earth is computed as

$$\bar{r}(t)_{sc/E} = |\bar{r}(t) - \bar{r}_E| \tag{9}$$

where

$$\bar{r}_E = [-\mu \;\; 0]^T. \tag{10}$$

The local minima of $r(t)_{sc/E}$ for $t \in [0, 2\pi]$ represent close approaches to Earth called perigees. For trajectories attaining multiple perigees during the month-long propagation period, only the absolute minimum pass-distance is recorded such that

$$r_p = min(r(t)_{sc/E}). \tag{11}$$

We identify trajectories of interest when r_p is located at or below the radius of GEO, indicating that the trajectory intercepts Earth-orbit (potentially one of the desired Earth-orbit destinations selected in Table 2). For trajectories satisfying $r_p \leq r_{GEO}$, we plot r_p as a function of Δv_1 and θ. By plotting this data, we are able to identify constraints on the magnitude and direction of Δv_1 required for attaining Earth-orbit from L_3-L_5.

Furthermore, we flag trajectories with r_p intersecting the relevant GEO, MEO, LEO radii, r_{orbit}, such that

$$|r_p - r_{\text{orbit}}| < \varepsilon. \tag{12}$$

where the tolerance is $\varepsilon = .003 * r_{\text{orbit}}$. These flagged trajectories will be examined in Step 4.

Step 4: Apply impulsive-maneuver to circularize trajectory into Earth-orbit

At perigee a second impulsive maneuver, $\Delta\bar{v}_2$, is used to circularize the transfer trajectory into Earth-orbit. Typically, computation of a velocity change at perigee involves only the magnitude difference between the pre- and post-burn vectors (written in the same coordinate frame) is needed. However, Step 4 formulates the full-form vector difference to account for a coordinate frame difference between our pre- and post-burn velocity vectors.

Recall that $\Delta\bar{v}_2$ is an impulsive maneuver transferring the spacecraft from a cislunar trajectory with $\bar{v}_p$ written in the CR3BP rotating frame to an Earth-orbit with $\bar{v}_{\text{orbit}}$ written in the inertial frame. A velocity vector in the CR3BP rotating frame (R) can be expressed with respect to the inertial frame (N) using the transport theorem

$$\begin{aligned} {}^N\bar{v}(t) &= \frac{{}^N d}{dt}(\bar{r}(t)) && (13)\\ &= \frac{{}^R d}{dt}(\bar{r}(t)) + \omega_{R/N} \times {}^R\bar{r}(t) && (14)\\ &= {}^R\bar{v}(t) + \bar{\omega}_{R/N} \times {}^R\bar{r}(t) && (15) \end{aligned}$$

where $\bar{\omega}_{R/N} = [0,\ 0,\ 1]^T$ n.d. (out-of-plane direction) is the angular rotation rate of the CR3BP rotating frame relative to the inertial frame.

Applying the transport theorem, the velocity change required by the second impulsive maneuver is computed as

$$\Delta\bar{v}_2 = \bar{v}_{\text{orbit}} - (\bar{v}_p + \bar{\omega}_{R/N} \times \bar{r}_p). \tag{16}$$

The total velocity change required to perform the cislunar transfer from the Lagrange Point to Earth-orbit sums the magnitudes of the first and second impulsive maneuvers

$$\Delta v_{\text{tot}} = \Delta v_1 + \Delta v_2. \tag{17}$$

We plot Δv_{tot} versus TOF to provide a comparison between cislunar transfers from L_3-L_5 to a desired Earth-orbit destination selected from Table 2.

3.2 Survey Trajectories Offering Transfers to the Desired Earth-Orbit

The values of Δv_{total} and TOF are quantitative measures for evaluating a transfer's fuel-efficiency and timely maneuverability. In mission design, transfers offering minimum Δv_{total} or minimum TOF are preferred. Plotting Δv_{total} versus TOF helps to better understand the tradespace of costs associated with transfers available from $L_3 - L_5$ to the Earth-orbit domain. From this plot, we are able to identify families of minimum Δv_{total} and minimum TOF transfers, each family consisting of 5-10 trajectories. Spatially plotting these families then provides a geometric understanding of the cislunar pathways spacecraft are likely to travel when transferring from the LPs to Earth-orbit.

4. RESULTS

4.1 Δv_1 Magnitude and Direction Constraints for Attaining Earth-Orbit from the Lagrange Points

Plotting r_p as a function of Δv_1 and θ in Figures 3, 5 and 7 shows that Earth-orbit can only be attained when applying certain magnitudes and directions of the $\Delta \bar{v}_1$ impulsive maneuver. The minimum values of Δv_1 required to reach Earth-orbit from L_3, L_4 and L_5 are given in Table 3. These values correspond to the darkest blue contour curve on each plot. All values of Δv_1 between this respective minimum and the maximum tested value 0.8 DU/TU produce trajectories that intercept Earth-orbit. Table 4 identifies limited ranges of θ, unique to the Lagrange point trajectories depart from, for which the Earth-orbit domain is intercepted. These ranges correspond to the minimum to the maximum departure angle recorded by each contour plot. While Figures 5 and 7 contain multiple sections or bands of contour curves, an absolute maximum and absolute minimum departure angle can still be determined. (Note that the departure angles from L_4 in Figure 3 have been wrapped from [-180 180] degrees and the departure angles from L_3 and L_5 in Figures 5 and 7 have been wrapped from [0 360] degrees.)

Using the minimum Δv_1 values and reduced θ ranges found, we can reduce the grid search size by approximately half for each Lagrange point. Thus, reducing computation time by eliminating parameter values for which Earth-orbit was not attainable.

LP of Origin	Min Δv_1, km/s
L_4	0.347878
L_5	0.337646
L_3	0.429732

Table 3: Minimum Δv_1 required to perform transfers from the respective Lagrange point to Earth-orbit.

LP of Origin	θ Range, degrees	$\Delta\theta$, degrees
L_4	[-78.68, 44.09]	122.77
L_5	[106.43, 275.98]	169.55
L_3	[23.78, 167.77]	143.99

Table 4: Range of θ enabling transfers to Earth-orbit from the respective Lagrange point. $\Delta\theta$ calculated to show spread of the range values.

The minimum Δv_1 values and θ ranges, shown in Tables 3 and 4, are found strictly for a time of flight limited to 2π TU and a maximum tested Δv_1 of 0.8 DU/TU. Increasing the assumed maximums for TOF duration or delta-v will alter these values; an investigation into how significantly the data will adjust has been left for future work.

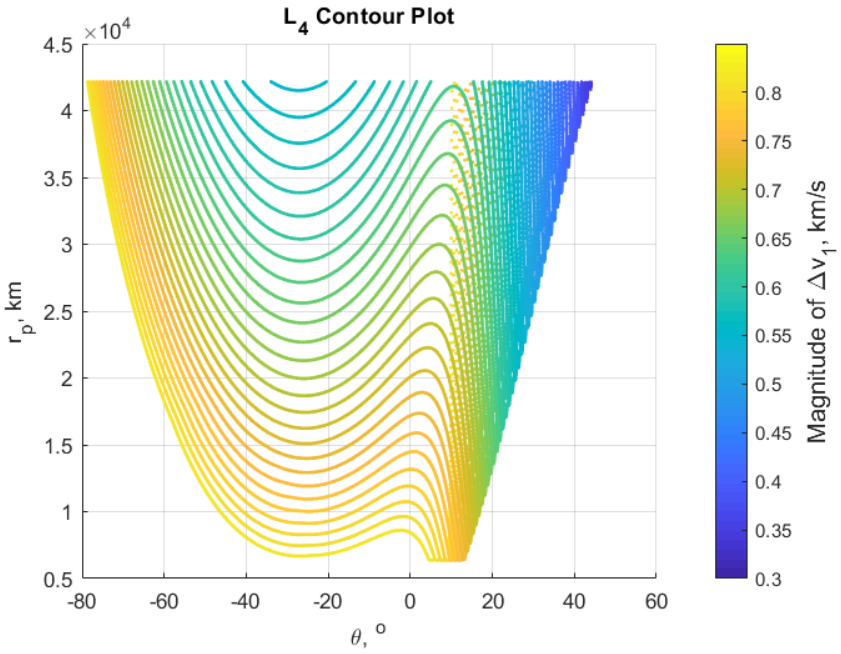

Fig. 3: L_4 perigee distances as a function of the magnitude of Δv_1 and departure angle θ.

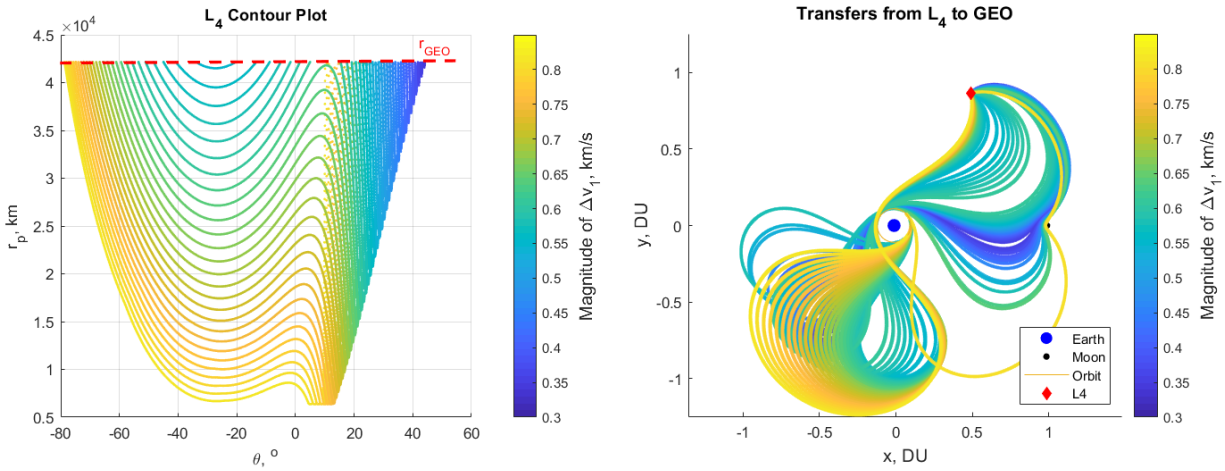

(a) Draw line at r_{GEO}

(b) Corresponding trajectories from L_4 to GEO

Fig. 4: The set of points along the horizontal black line $r_p = r_{GEO}$ represent the parameter set $(\Delta v_1, \theta)$ for trajectories intersecting GEO.

Each contour plot depicted in Figures 3, 5 and 7 presents a patterned structure of sequential, enveloping curves that plot r_p as a function of Δv_1 and θ. The plotted r_p range from 6,738 km to 42,164 km – the radius at Earth's surface to GEO. By selecting a perigee radius according to a desired Earth-orbit destination, the set of all possible parameters Δv_1 and θ for attaining that orbit are provided by (1) drawing a horizontal line across the contour plot at the desired r_p value and (2) finding points of intersection between the contour curves and line drawn (as shown in Figure 4).

The L_4 contour plot in Figure 3 shows the smoothest continuation from one contour curve to the next forming a single wedge in the shape of a skewed "W". A "flat-lining" phenomenon, which occurs on all three contour plots, disrupts the structure presented by the contour curves. Occurring at $r_p = 6,378$ km, the "flat-line" indicates instances where trajectories have been terminated upon impacting the Earth, their perigees thus measured as Earth's average radius.

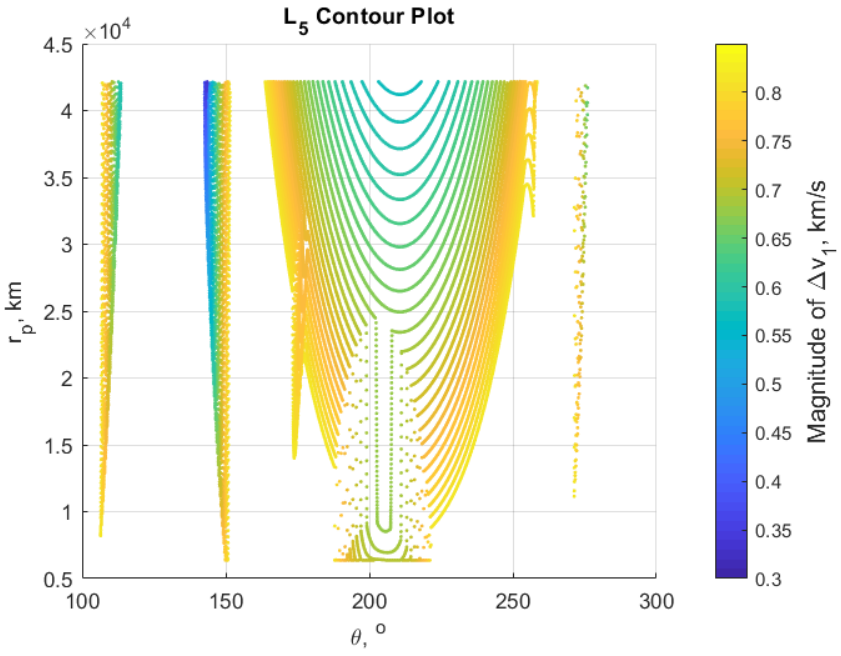

Fig. 5: L_5 perigee distances as a function of the magnitude of Δv_1 and departure angle θ.

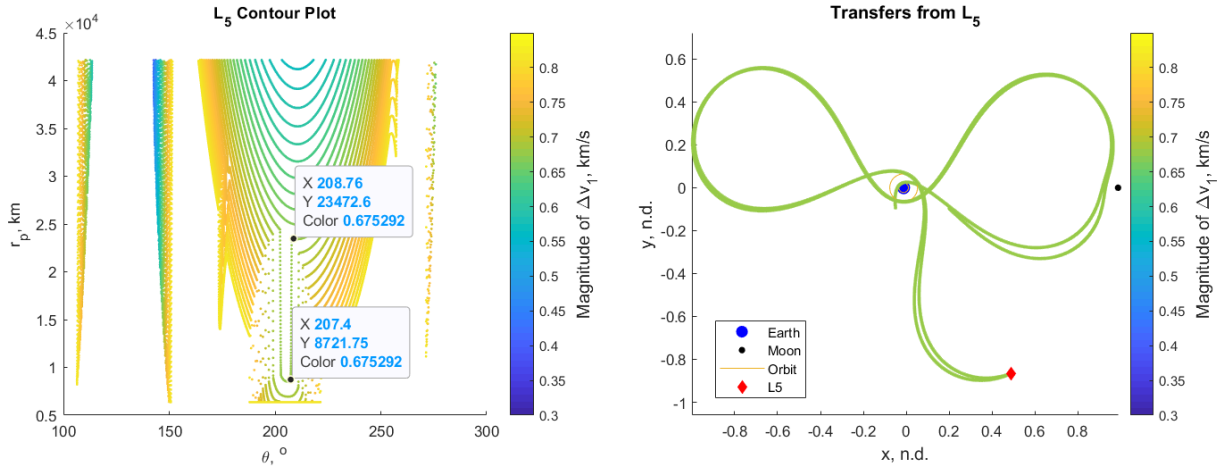

(a) Points of interest

(b) Corresponding trajectories from L_5

Fig. 6: The minimum perigee radius is dependent on the maximum allowed transfer duration.

Trajectories originating from L_5 attain Earth-orbit for four distinct groupings of departure angles (Figure 5). Additionally, it can be noted that the lowest magnitudes of Δv_1 occurred for departure angles in the 142-145° range. The abrupt dip in the contour curves seen for approximately $r_p < 2{,}500$km and $185^\circ < \theta < 225^\circ$ is due to trajectories that attain a low-altitude, third perigee within the 2π TU maximum flight duration while other trajectories only complete two higher altitude close approaches with Earth before the maximum time of flight terminates trajectory propagation. An example of this is illustrated in Figure 6 – two trajectories having similar Δv_1 parameterization (i.e. $\Delta v_1 = 0.675292$ km/s; $\theta \in (207.40^\circ, 207.87^\circ)$ are propagated for the maximum flight duration. While the trajectories travel along similar pathways, only one completes a third perigee within the month-long time of flight. This third perigee occurs at an approximate 8,700-km radius in comparison to the previous 23,500-km perigees. Being the absolute minimum radius of perigee, this third perigee is recorded on the contour plot for such trajectories. The key take-away from this example is that the absolute minimum perigee attained along a transfer is dependent on the allowed maximum TOF.

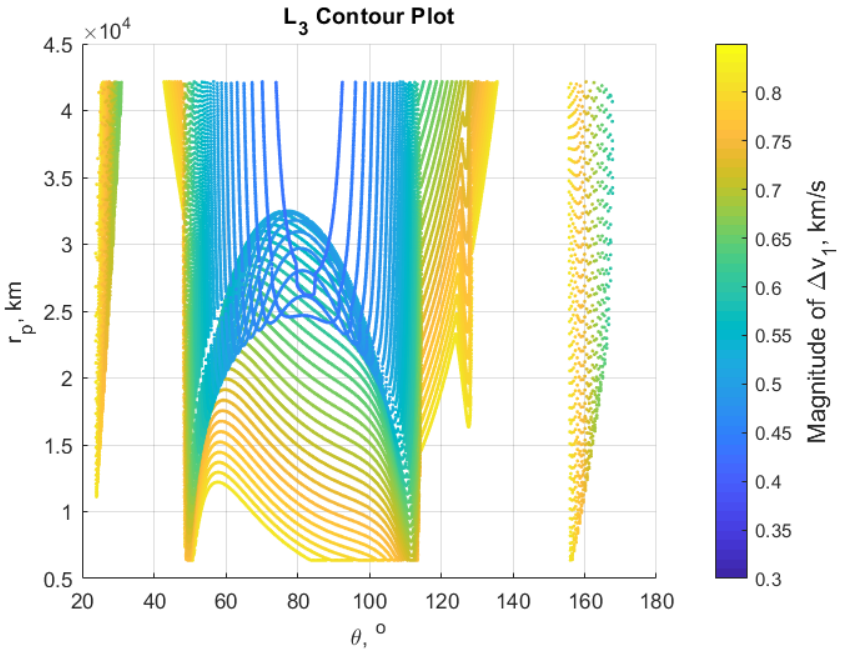

Fig. 7: L_3 perigee distances as a function of the magnitude of Δv_1 and departure angle θ.

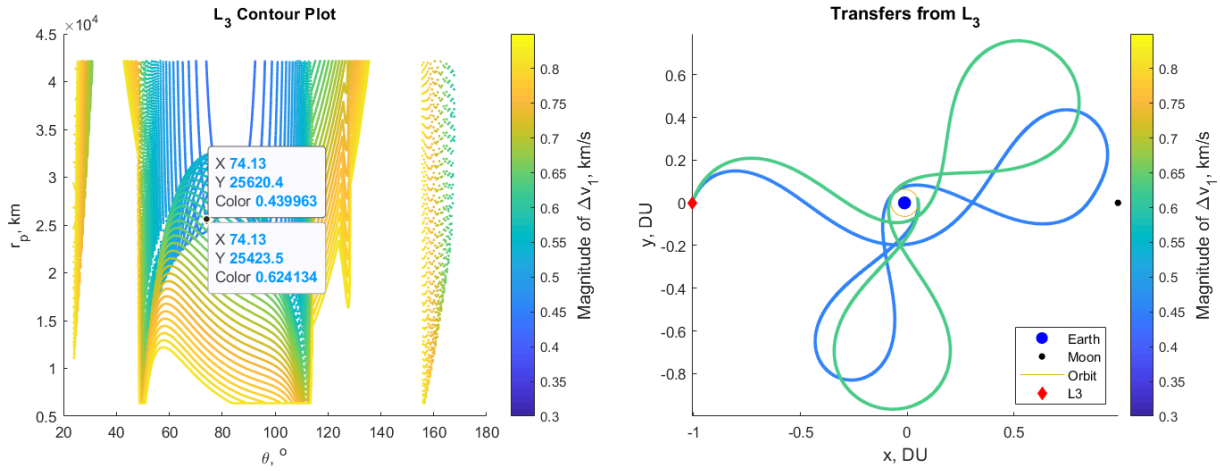

(a) Point of intersection

(b) Corresponding trajectories from L_3

Fig. 8: Intersection points on the contour plots identify two solutions for transferring to the same Earth-orbit.

The L_3 contour plot in Figure 7 shows three groupings of departure angles - the center section featuring curves which overlap one another. Points of intersection between contour curves identify where differing magnitudes of Δv_1 from the same departure angle, θ, result in the same r_p. Figure 8 provides an example of how two trajectories, originating from L_3 with $\theta = 74.13^\circ$ but having different impulsive maneuver magnitudes, can provide different transfer options to Earth-orbits within 3-km radial distance of each other. In this case, the difference of approximately 184 m/s imparted along the same departure angle resulted in geometrically similar trajectories. However, it should be noted that minimal differences in Δv_1 magnitude or direction can result in significant variation between the spatial pathways traveled by the corresponding trajectories.

4.2 Minimum-Δv_{tot} and Low-TOF Transfer Families

In the realm of trajectory design, the primary measures of cost associated with performing a trajectory transfer are Δv_{tot} and TOF. Both of these measures factor into the strategic value and applications of trajectory transfers. Trajectories having lower Δv_{total} are more fuel-efficient allowing a spacecraft to allocate a greater fraction of its fuel-reserve for mission operations once arriving to the orbit destination. Defining what constitutes a timely transfer is often mission-dependent. The results of this section examine the Δv_{tot} and TOF costs associated with performing transfers between the selected Lagrange points and desired Earth-orbits.

The results of this section have been grouped by Earth-orbit destination: GEO, MEO, or LEO, rather than by a trajectories' originating Lagrange point. This is done to aid in the visualization of results for mission planning purposes. We are exploring transfers that enable storage of a spacecraft at one of the Lagrange points to replenish satellite constellations in operation around Earth. In this regard, the destination orbit of the transfer is arguably more important than the trajectory's starting location. For example, a transfer delivering a telecommunications satellite intended to replace a non-operational spacecraft on-orbit in GEO must arrive to the GEO-belt. A satellite's orbit of operation is a mission requirement while its storage location is open for selection based on time of flight or Δv_{tot} constraints allotted for the transfer.

For each Earth-orbit destination, Table 5, records Δv_{tot} and TOF pairings corresponding to the absolute minima of these quantitative measures. The values displayed by the table have been gathered from Figures 9a, 9c and 9e. Recall that these results are constrained by a month-long maximum TOF and a 0.8 DU/TU $\approx$ 0.81854 km/s maximum for Δv_1.

Destination	Optimality	L_3	L_4	L_5
GEO	min-Δv_{tot}	(1.46449, 19.7512)	(1.36149, 26.7778)	(1.36701, 24.9810)
	min-TOF	(1.90292, 3.5434)	(1.69679, 15.7083)	(1.90757, 3.5813)
MEO	min-Δv_{tot}	(1.80169, 27.2911)	(1.88148, 23.7571)	(1.9462, 26.4517)
	min-TOF	(2.15963, 7.4478)	(2.19688, 14.9020)	(2.25213, 3.6572)
LEO	min-Δv_{tot}	(3.59238, 27.1214)	(3.64161, 19.8987)	(3.60083, 26.9225)
	min-TOF	(3.70308, 18.1813)	(3.74874, 4.6078)	(3.74517, 26.2992)

Table 5: Optimal transfers listed by their (Δv_{tot} [km/s], TOF [days]) costs. Grouped by the Lagrange point of origin and Earth-orbit destination for the transfer, each cell of the table contains both the minimum Δv_{tot} and minimum TOF transfers for side-by-side comparison.

GEO Transfers: Considering the trajectories that provide transfers to GEO from each Lagrange point, transfers from L_3 or L_5 offer the shortest TOF, ranging from about 3-4 days, with comparable Δv_{tot} costs on the order of 1.90 km/s. Least expensive transfers are available from L_4 and L_5, on the order of 1.36 km/s, but compromise increased fuel-efficiency for a longer transfer time of 3-4 weeks. Transfers from L_5 to GEO include both minimum Δv_{tot} and minimum TOF options. Enabling the selection of a trajectory that minimizes either Δv_{tot} or TOF from the same Lagrange point is advantageous; this allows mission planning to account for both time-critical and fuel-limited scenarios when returning to Earth-orbit. This is especially true as there is an approximate 540 m/s difference between the impulsive maneuvers required to perform the minimum Δv_{tot} and minimum TOF solutions from L_5 to GEO.

MEO Transfers: Transfers arriving to MEO from L_5 can be completed in approximately three-and-a-half days at the cost of 2.25 km/s to perform the two impulsive velocity changes. Transfers from L_3 offer the lowest Δv_{tot} of 1.80 km/s but take four weeks to complete. L_4 to MEO transfers feature median Δv_{tot} costs and TOF durations, and may not be optimal solutions. MEO transfers will need to chose between the TOF or delta-v mission requirement as being most imperative to the mission.

LEO Transfers: Entering into LEO from the Lagrange points is the most fuel-demanding maneuver sequence when comparing transfers to the three Earth-orbit destinations. Performing these transfers costs between 3.59-3.75 km/s, having varied flight durations. The fastest LEO transfer originates from L_4 and is completed in 4.6 days requiring approximately 3.75 km/s. The absolute minimum Δv_{tot} occurs for transfers from L_3 completed in 27.3 days. The delta-v difference between the minimum Δv_{tot} and TOF solutions from each Lagrange point range from 107-144 m/s. Selection of a transfer to LEO, will likely be driven by TOF constraints and spatial geometry of the trajectory in accordance with mission requirements for the transfer rather than delta-v constraints.

Overall, selection of a minimum TOF versus a minimum Δv_{tot} transfer will need to consider the additional 0.150-0.540 km/s cost required to reduce the 3-4 week transfer duration of the absolute minimum Δv_{tot} solution to the 3-5 day transfer duration of the absolute minimum TOF solution.

4.3 Surveying the Spatial Representation of the Transfer Families

While the preceding subsection discussed the absolute minimum TOF and Δv_{tot} solutions for completing transfers from the Lagrange points to Earth-orbit, it should be noted that these solutions only encompass a select few of the total trajectory options for attaining Earth-orbit. Figures 9b, 9d and 9f show the minimum TOF or minimum Δv_{tot} families, colored according to value of their Δv_{tot} cost, as a subset of the complete set of transfers to the desired orbit, colored in grey. For Δv_{tot} or TOF requirements featuring intermediary values, the graphs displayed in Figures 9a, 9c and 9e are tools for comparing and finding suitable trajectories to meet delta-v or TOF requirements.

The collection of minimum-Δv_{tot} and minimum-TOF families identified in the previous subsection produce an assortment of spatial trajectories for traveling from the three selected Lagrange points to a desired Earth-orbit. Examining the regions of cislunar space through which these trajectories travel and their spatial geometries, we can identify qualitative characteristics and patterns attributed to each transfer family.

In Figure 9, we see that all transfers inject into prograde Earth-orbit. This is due to the maximum TOF and Δv_1 range limit imposed during the grid search for solutions. A higher magnitude of Δv_1, and likely a longer TOF, would be needed to search for potential retrograde orbit solutions.

The shortest-TOF trajectories can be geometrically identified by the "S"-shaped paths passing directly between the respective Lagrange point and Earth-orbit radius (orbit marked in yellow) in Figure 9. An easy way to locate these transfers on the spatial plots is to draw an imaginary line from the Lagrange point to Earth and identify the skewed "S"-shaped trajectories centered about that line. These minimum-TOF transfers only attain one perigee, at which a circularizing maneuver injects the spacecraft into Earth-orbit.

The minimum Δv_{tot} transfers travel along less-direct paths to reach Earth-orbit from the Lagrange points. These trajectories form lobes surrounding the Earth, often attaining 2-3 perigee before intersecting the desired Earth-orbit radius to within the ε tolerance. For trajectories arriving to GEO and MEO, the first close approach to Earth is just outside the GEO or MEO radius and must make a second pass before obtaining perigee at the exact desired Earth-orbit radius. In these cases, corrective maneuvers could be used to prematurely intersect with the desired GEO or MEO orbit upon the first perigee, rather than waiting for the second perigee, if time is critical. This observation does not hold for the LEO transfers. Their initial close approaches to Earth are high-altitude passes not in the vicinity of LEO.

We also see the tendency for a subset of the minimum Δv_{tot} transfers, those originating from L_4, to travel through lunar vicinity (see Figures 9b, 9d and 9f). These trajectories attaining gravity-assisted close approaches to the moon before being redirected towards Earth. Such transfers would enable mission operations in lunar vicinity (potentially entering and departing lunar orbit) before continuing on to arrive at the respective Earth-orbit destination.

4.4 Example Mission Planning Application

The strategic value of certain trajectories over others will be application dependent - balancing the time of flight requirements and propellant budget allotted for the trajectory transfer. For example, say a repository of backup satellites was placed in storage at one of the Lagrange points, at the ready to replace communications satellites rendered non-operational on-orbit in GEO. In the event that a satellite unexpectedly ceases functional operation, a fast transfer time enabling rapid replacement would be preferred. On the other hand, a scheduled satellite replacement occurring at end-of-life would require a less urgent transfer time and prioritize low fuel cost. Placing such a repository of replacement satellites in storage at L_5 would enable both mission scenarios.

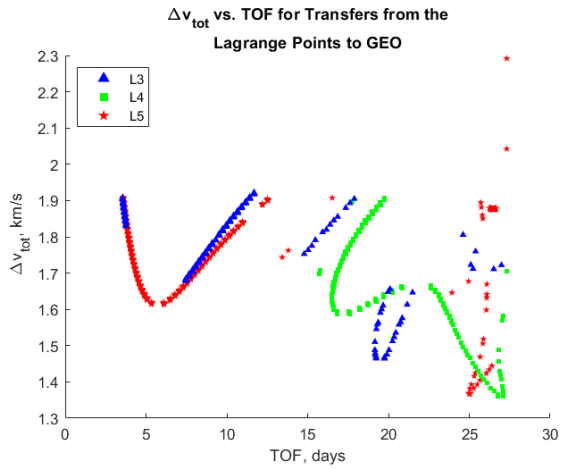

(a) Δv_{tot} versus TOF for transfers to GEO.

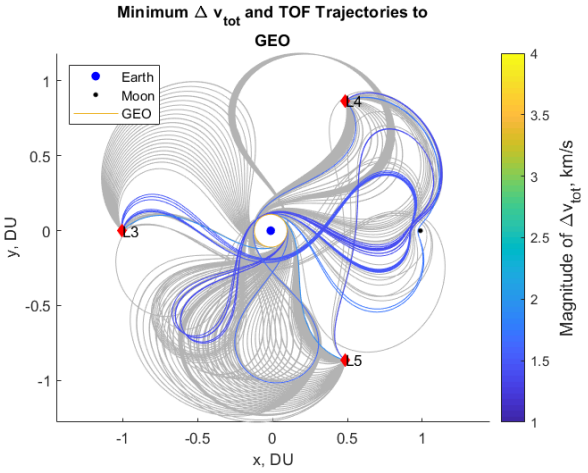

(b) Minimum Δv_{tot} or minimum TOF transfers from L_3-L_5 to GEO.

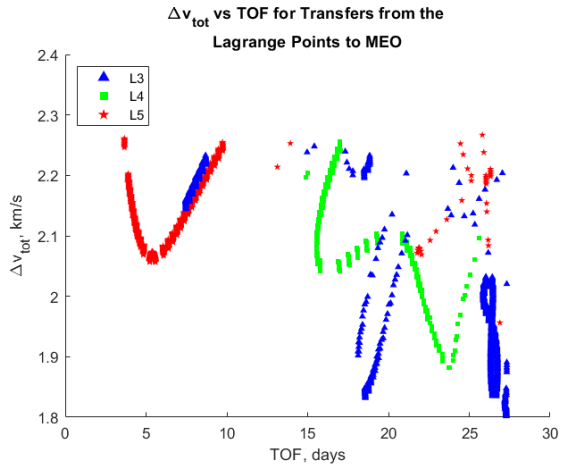

(c) Δv_{tot} versus TOF for transfers to MEO.

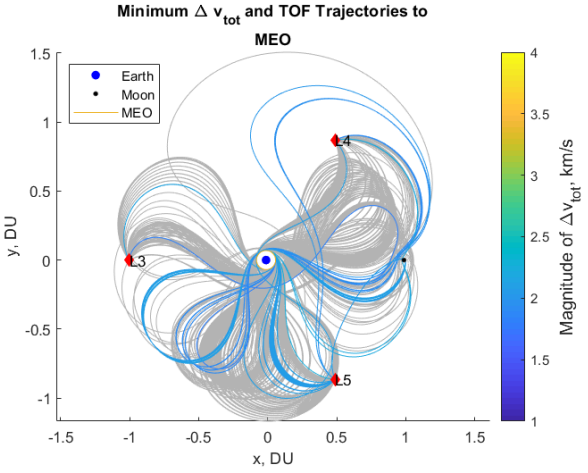

(d) Minimum Δv_{tot} or minimum TOF transfers from L_3-L_5 to MEO.

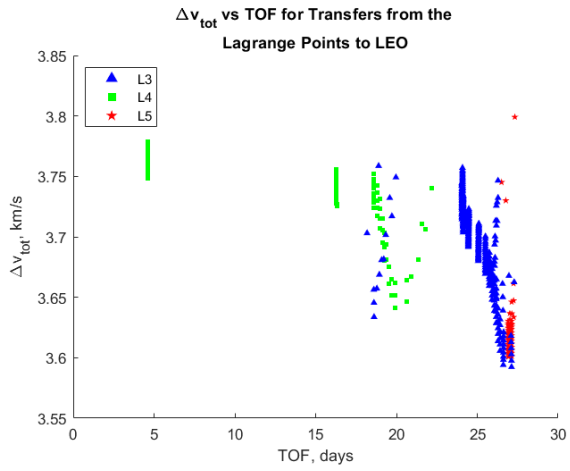

(e) Δv_{tot} versus TOF for transfers to LEO.

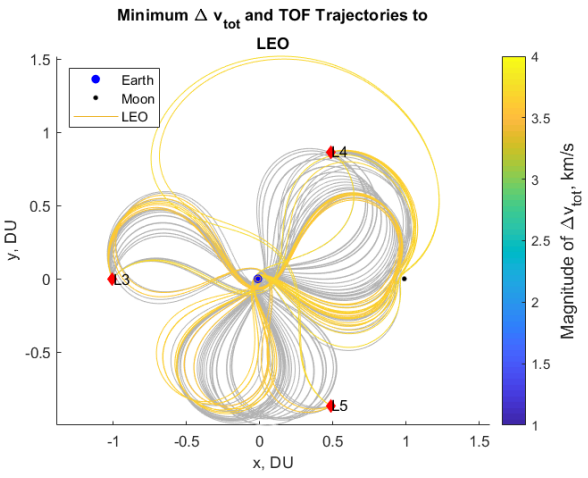

(f) Minimum Δv_{tot} or minimum TOF transfers from L_3-L_5 to LEO.

Fig. 9: The left column of figures provides a comparison of Δv_{tot} versus TOF for attaining each Earth-orbit at GEO, MEO or LEO. The right column of figures spatially represents the minimum Δv_{tot} or minimum TOF transfers, colored according to their Δv_{tot} cost. Trajectories in grey do not represent these minimums but still offer a transfer from Lagrange point to Earth-orbit. In Figure 9c, value at (27.3215, 5.58701) omitted. In Figure 9e, values at (27.3215, 9.34059), (27.3215, 5.94314), (27.3215, 5.34989), and (27.3215, 5.21998) omitted.

5. CONCLUSION

This investigation analyzed two-impulse transfers returning a spacecraft from the L_3, L_4 and L_5 regions to Earth-orbit. The magnitude and direction of the initial impulsive maneuver applied at the Lagrange point determines the radius of Earth-orbit that the transfer will intercept and circularize into. Plotting minimum TOF and minimum Δv_{tot} transfer families revealed geometric characteristics of the families and common pathways traveled through cislunar space from the Lagrange points to Earth-orbit.

Future work will map three-dimensional corridors of travel existing in cislunar space by expanding analysis into the full CR3BP dynamics model and implementing continuation methods such as Monte Carlos research. Applied to cislunar architecture design, this work becomes beneficial to space situational awareness and space traffic management. The volume of cislunar space is vast – monitoring and tracking satellites across this region takes time and resources. These corridors of travel, characterized as low-cost routes for traveling between regions in the Earth-Moon system, identify sub-volumes of cislunar space where spacecraft are most likely to be located. We can focus and refine the overall volume of space an observer satellite must monitor in order to perform target tracking in the cislunar domain.

Additionally, grouping of the minimum Δv_{tot} and minimum TOF transfer families could be improved by incorporating clustering algorithms. The trajectory design process could be made more realistic through the inclusion of low-thrust maneuvers used to assist circularizing the trajectory into Earth-orbit.

REFERENCES

[1] Kathryn Davis, George Born, and Eric Butcher. Transfers to Earth-Moon L3 halo orbits. *Acta Astronautica*, 88:116–128, 2013.

[2] David Folta and Frank Vaughn. A Survey of Earth-Moon Libration Orbits: Stationkeeping Strategies and Intra-Orbit Transfers. In *AIAA/AAS Astrodynamics Specialist Conference and Exhibit*, page 4741, 2004.

[3] Dawn Perry Gordon. Transfers to Earth-Moon L2 Halo Orbits. Master's thesis, Master Thesis of Science in Aeronautics and Astronautics, Purdue University . . . , 2008.

[4] Marcus J Holzinger, C Channing Chow, and Peter Garretson. A primer on cislunar space. 2021.

[5] M Klonowski, NO Fahrner, C Heidrich, and M Holzinger. Robust Cislunar Architecture Design Optimization for Cooperative Agents. In *Proceedings of the Advanced Maui Optical and Space Surveillance (AMOS) Technologies Conference*, page 15, 2023.

[6] Michael Klonowski, Marcus J Holzinger, and Naomi Owens Fahrner. Optimal Cislunar Architecture Design using Monte Carlo Tree Search Methods. *The Journal of the Astronautical Sciences*, 70(3):17, 2023.

[7] Slim Locoche, Rémi Delage, Philippe Leblond, Waldemar Martens, Lorenzo Bucci, Jessica Grenouilleau, and Salvatore Vivenzio. Cis-lunar Transfer Vehicle: Mission Analysis for an ESA Transfer Vehicle to the Gateway. *ESA GNC-ICATT*, 2023.

[8] Raoul R. Rausch. Earth to Halo Orbit Transfer Trajectories. Master's thesis, 2005.

[9] Jing Ren, Youliang Wang, Mingtao Li, and Jianhua Zheng. A trajectory design and optimization framework for transfers from the Earth to the Earth-Moon triangular L4 point. *Advances in Space Research*, 69(2):1012–1026, 2022.

[10] John E Shaw, Jean Purgason, and Amy Soileau. Sailing the New Wine-Dark Sea. *Aether: A Journal of Strategic Airpower & Spacepower*, 1(1):35–44, 2022.